

Effective Kidney Stone Prediction Based on Optimized Yolov7 Segmentation and Deep Learning Classification

B. Reuben*¹ and C. Narmadha²

Submitted: 18/08/2023

Revised: 11/10/2023

Accepted: 23/10/2023

Abstract: Recently, the most common urological disease is Kidney stones that affect most of the individuals globally which provides a severe pain and discomfort. The kidney stone prediction is must for effective treatment planning and patient care. In this work, the Deep learning model of YOLO v7 model based Energy Valley optimizer for image segmentation and Pulse Couple Neural Network (PCNN) based classification is proposed effective approach for kidney stone prediction. At first, the YOLO v7 model is identified and localized the kidney stones for image segmentation. However, to provide an optimal result in YOLOv7 performance, the hyperparameter tunings are performed to learn and generalize from data. To achieve an optimal result, the Energy Valley optimizer is introduced that is motivated by energy valleys found in physics. This optimizer efficiently searches for optimal hyperparameters, mitigating issues such as local optima and slow convergence. By combining the YOLO v7 model with the Energy Valley optimizer, it enhances the model's predictive capabilities and improves an accurate segmentation of kidney stones. Furthermore, the Pulse Couple Neural Network (PCNN) method is presented classification framework to classify kidney stones based on their attributes. The PCNN model leverages the temporal dynamics of pulse-coupled oscillators to capture complex patterns and relationships within the segmented kidney stone regions. This facilitates accurate classification into different stone types, aiding in personalized treatment planning. In experiment, the proposed technique has achieved remarkable results across various evaluation metrics such as precision, recall, accuracy, F1 score and specificity values of 98.58%, 99.17%, 98.88%, 97.42%, and 98.23% respectively. These metrics demonstrated exceptional accuracy in detecting and classifying kidney stones than the other traditional techniques. The proposed model has validated the effectiveness and superiority of the proposed technique for kidney stone prediction.

Keywords: Kidney stone, Image Segmentation, YOLOv7 model, Energy Valley optimizer, PCNN classification, performance metrics.

1. Introduction

Kidney stones are also named as renal calculi that are salt deposits and solid mineral formed within the kidneys. It provides an excruciating discomfort and pain when it obstructs the urinary tract. Kidney stones are a prevalent urological condition, affecting a substantial number of individuals worldwide [1]. The timely and accurate prediction, segmentation, and classification of kidney stones play a vital role in guiding effective treatment strategies and improving patient outcomes.

There are various types of kidney stones namely calcium oxalate stones, uric acid stones, calcium phosphate stones and struvite stones [2]. For every kidney stone disease has unique characteristics and also need specific treatments. Based on treatment planning and management, the kidney stones are identified accurately and provided better classifications [3].

The main issue in kidney stones is the lack of early prediction. Because many more time the stones are very painful after it become larger that also caused many complications. Due to this delay detection and diagnosis can

lead to severe pain, urinary tract infections, and sometimes the kidney can also damage [4]. Whereas the Earlier prediction can help in appropriate interventions, preventing form a complications, and enhancing the patient outcomes. To avoid such issues, the Deep learning (DL) methods are presented in medical image analysis. The DL methods can perform an effective kidney stone segmentation and classification for earlier prediction [5]. For such kidney stones classification, the DL model can perform by training on labeled datasets, these models can learn to differentiate between calcium oxalate stones, uric acid stones, and other types based on their unique characteristics, such as shape, texture, and composition [6]. Accurate classification aids in determining the appropriate treatment approach and helps healthcare professionals make informed decisions. In the DL methods, Convolutional neural networks (CNNs) have been widely employed for accurate segmentation of kidney stones within medical images [7]. These techniques leverage the ability of CNNs to learn discriminative features and localize objects of interest, enabling precise identification and delineation of kidney stones. Likewise there are several CNNs variant methods are used for medical imaging such as InceptionNet, GoogleNet, AlexNet, ImageNet, Recurrent Neural Network (RNN), Long Short Term Memory (LSTM) respectively [8].

^{1,2}Periyar Maniammai Institute of Science & Tech, Thanjavur – 613403, Tamil Nadu, India.

ORCID ID : 0009-0001-2801-8849

*Corresponding author email id: princeton.reuben@gmail.com

In this study, it aims to address these challenges by exploring the potential of deep learning techniques, specifically focusing on segmentation and classification of kidney stones. It is aimed to contribute to the early detection and personalized treatment of this prevalent urological condition [9-11]. In this work, an accurate kidney stone prediction and classification is performed by integrating the YOLO v7 model with the Energy Valley optimizer for a segmentation technique, and the PCNN classification framework. It achieves superior performance and provides valuable insights into the characteristics of kidney stones. This advancement in predictive modeling can contribute to personalized treatment planning and improve healthcare outcomes for individuals with kidney stones.

2. Related Works

In the field of kidney disease diagnosis and kidney stone detection, various studies have utilized deep learning and machine learning techniques. Shi et al. [12] presented a segmentation based on fully automatic for kidney images, employing pre-trained CNN to extract relevant features. In [13], the new deep learning model with adaptive weighting score is used to predict a chronic kidney disease. Abdullah et al. [14] focused on early detection of chronic kidney disease (CKD) based on artificial neural networks (ANN) and support vector machines (SVM) techniques.

Yildirim et al. [15] developed a DL based coronal CT scans for kidney stone prediction. It is used to analyze severity based on image features to provide an accurate detection even the stone was small. Baygin et al. [16] developed ExDark19 for an image classification method using CT images. It employed iterative neighbourhood component analysis for feature selection and an AdaBoost classifier for stone identification with an accuracy of 88.9% respectively.

Homayounieh et al. [17] explored a renal calculi prediction using autosegmentation-assistance. Next, Alnazer et al. [18] presented a survey work for monitoring renal function decline that highlights the DL performance in improving renal dysfunction monitoring and prediction. Patro et al. [19] developed DL architecture using CNN model by achieving impressive accuracy in kidney stones prediction from CT images. Similarly, Yildirim et al. [20] presented an automated system using DL for kidney stone detection with a high accuracy even for small-sized stones. These studies highlight the potential of DL approaches with a high diagnostic accuracy and patient care in renal imaging and kidney stone detection.

Akshaya et al. [21] used a Back Propagation Network (BPN) with Fuzzy C-Mean (FCM) clustering for kidney stone detection, while Mua'ad et al. [22] explored three segmentation techniques (threshold-based, watershed-based, and edge-based) to enhance kidney stone detection. Additionally, Goel et al. [23] presented an improved kidney

stones from ultrasound images by using Gray-Level Co-occurrence Matrix (GLCM) features for performance evaluation. These studies highlight the segmentation methods and classification algorithms to improve accuracy and image quality.

3. Materials

Dataset Description

The study utilized a dataset of coronal CT scans obtained from a publicly available kidney stone detection repository on GitHub (https://github.com/yildirimozaal/Kidney_stone_detection). This dataset includes scans from different institutions and scanners, aimed at developing intelligent algorithms for stone segmentation and classifications. The CT scans, acquired in DICOM format, were pre-processed to ensure patient privacy. The dataset consists of CT scans from male and female patients, aged 17 to 79 years, diagnosed with kidney stones by radiologists or urologists. Rigorous review and annotation by at least two radiologists were conducted to create a reliable dataset with scans. Among these, 5077 were from normal subjects, Cyst 3,709, stone 1,377, and tumor 2,283. The dataset was primarily collected from a hospital in Turkey, focusing on urinary system stone disorders. CT scans are known for their high sensitivity in detecting kidney stones.

4. Proposed Methodology

The figure 1 shows the proposed workflow for kidney stone prediction. It consists of several processes such as: Data Acquisition that is used to obtain a dataset of kidney stone images in DICOM format and contains a diverse range of images from different sources, Data Preprocessing that is used to preprocess the dataset by removing any personal identification data and standardizing the images to ensure consistency, Image Segmentation is done by using the trained YOLOv7 model to segment the kidney stone regions within the images. It can accurately identify and localize the kidney stones. Also, the Energy Valley Optimization is applied to fine-tune the hyperparameters of the YOLOv7 model for an improved speedy performance and higher accuracy, then the Image Classification is done by PCNN that is used to provide accurate predictions based on patterns in the data and finally the Model Evaluation is performed based on the metrics such as accuracy, precision, recall, and F1 score to measure the effectiveness of the model.

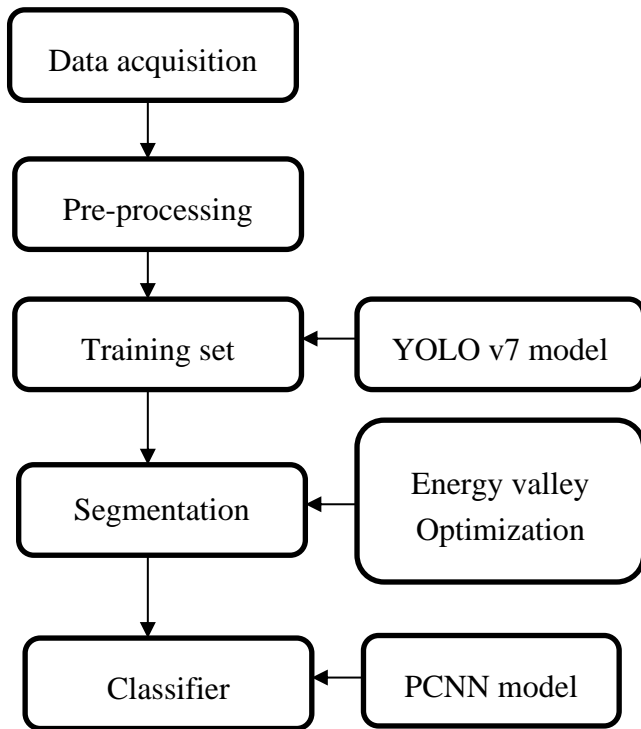


Fig.1. Proposed Workflow

By following this workflow, the integrated system aims to provide accurate and efficient prediction of kidney stones using YOLOv7 for image segmentation and PCNN for classification.

4.1. Image Segmentation

The YOLOv7 architecture is a highly effective and widely used for image segmentation that is shown in figure 2. It comprises a several components such as Backbone Network, Feature Pyramid Network, Head and YOLO Loss respectively [24].

1. Backbone Network: The backbone network serves as the foundation of YOLOv7. It typically consists of a deep CNN namely Darknet-53 or ResNet. This network's primary function is to extract high-level features from the input image. It learns to recognize various patterns and shapes that are crucial for segmentation.

2. Feature Pyramid Network (FPN): FPN is integrated into YOLOv7 to address the challenge of detecting objects at different scales. It enhances the feature representation by combining features from different levels of the backbone network. FPN generates a feature pyramid, where each level of the pyramid corresponds to features at different resolutions. This allows YOLOv7 to effectively segment objects of various sizes and handle scale variations.

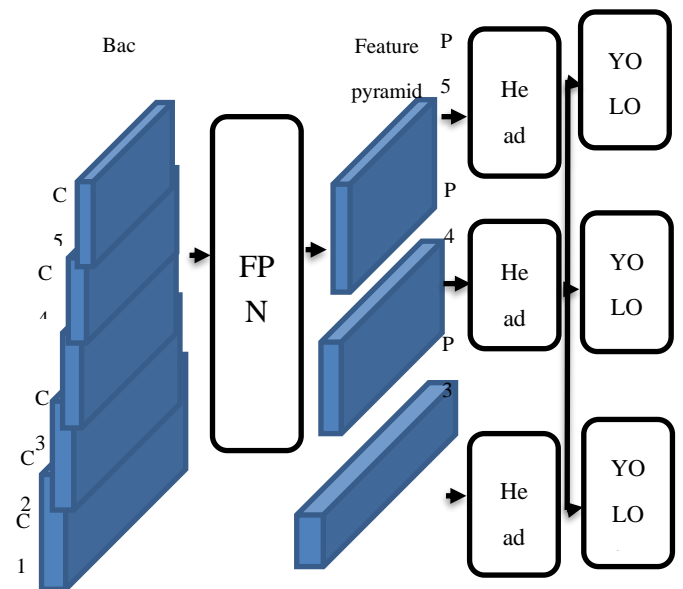


Fig 2. YOLO v7 Architecture

3. Feature Pyramid: The feature pyramid is the output of the FPN. It consists of multiple feature maps at different scales. These feature maps retain information from various levels of detail. The lower-level maps contain fine-grained details, while the higher-level maps capture more abstract and semantic information. The feature pyramid enables YOLOv7 to have an input image multi-scale representation that allowed to segment features at different resolutions.

4. Head: The head of the YOLOv7 architecture follows the feature pyramid. It processes the feature maps and generates predictions for bounding boxes and class probabilities. The head typically includes additional convolutional layers, which refine the features and extract more specific information about the objects. It predicts the bounding box coordinates and class labels for the detected objects within each feature map.

5. YOLO Loss: The YOLO loss function calculates the discrepancy between the predicted bounding boxes and class probabilities and the ground truth annotations. It consists of three main components:

- Localization Loss: This component measures the difference between the predicted and ground truth bounding box coordinates. It encourages accurate localization of objects.

- Confidence Loss: The confidence loss compares the predicted objectness scores (confidence scores indicating the presence of an object) with the ground truth labels. It guides the model to assign high confidence to correctly detected objects and low confidence to false detections.

- Class Loss: The class loss evaluates the difference between the predicted class probabilities and the ground

truth labels. It ensures accurate classification of objects into their respective classes.

By minimizing the YOLO loss during training, the model learns to make precise predictions of object locations and class labels.

Overall, the YOLOv7 architecture combines the backbone network, FPN, feature pyramid, head, and YOLO loss to achieve accurate and efficient object detection. It can process images in real-time and detect objects at different scales, making it suitable for various applications, including object recognition, segmentation, and tracking.

4.2. Hyperparameter of YOLOv7

The hyperparameters commonly used in training a YOLOv7 model, along with the number of epochs, include:

1. Learning Rate: Determines the step size for updating model parameters during training.
2. Batch Size: Specifies the number of training samples processed in each iteration.
3. Input Image Size: Defines the dimensions of the input images processed by the model.
4. Anchor Boxes: Predefined bounding boxes of different scales and aspect ratios for object localization.
5. Confidence Threshold: Minimum confidence score required for a detected object to be considered valid.
6. NMS Threshold: Minimum IoU overlap required for suppressing duplicate bounding box predictions.
7. Number of Epochs: Specifies the number of complete passes through the training dataset during training.

Here's an example of the hyperparameters and epochs is given in Table 1:

Table.1 Hyperparameter and possible values

Hyperparameter	Possible Values
Learning Rate	0.01
Batch Size	16
Input Image Size	608x608
Anchor Boxes	Custom configurations
Confidence Threshold	0.6
NMS Threshold	0.6
Number of Epochs	100

4.3. EVO Based Fine-Tuning

The Energy Valley Optimizer (EVO) is a novel metaheuristic algorithm that draws inspiration from advanced physics principles, particularly the stability and

decay modes of particles [25]. The algorithm has been proposed and evaluated using 20 unconstrained mathematical test functions in various dimensions to assess its performance.

In the EVO, particles are considered unstable and tend to decay, emitting energy in the process. The decay rate varies among different types of particles, and stability is determined by the number of neutrons (N) and protons (Z) and the N/Z ratio. The stability band is defined by the N/Z ratio, with a higher value indicating stability for heavier particles.

Particle stability is influenced by the neutron enrichment levels, with neutron-rich particles requiring more neutrons for stability and neutron-poor particles undergoing electron capture or positron emission to change towards the energy valley or stability band.

The decay process involves the emission of alpha (α) particles (helium-like particles), beta (β) particles (high-speed electrons), and gamma (γ) rays (high-energy photons). Alpha decay reduces the N/Z ratio, beta decay increases the N/Z ratio, and gamma decay involves emitting gamma photons without changing the N/Z values.

The EVO algorithm utilizes these principles of particle decay and stability to improve the search for optimal solutions in optimization problems. It employs higher-level searching techniques inspired by the decay process and the tendency of particles to reach a stable point. The algorithm starts with initial candidate solutions and gradually improves their overall standing through iterative steps.

Algorithm 1: pseudocode of EVO algorithm for hyperparameter tuning:

1. Initialize population of candidate hyperparameter configurations
2. Set maximum number of iterations or termination condition
3. While termination condition is not met do:
4. Evaluate the performance of each candidate configuration using a validation set or cross-validation
5. Update global best configuration based on performance values
6. For each candidate configuration do:
7. Select neighboring configurations based on a certain strategy
8. Update candidate configuration using the Energy Valley Optimization equations:
9. Compute binding energy based on stability criteria (e.g., performance ranking)
10. Adjust hyperparameter values to move towards stability or energy valley
11. Apply local search or mutation operator if necessary

12. Perform selection or elitism to determine new population of candidate configurations
13. End While
14. Return the best hyperparameter configuration found

From the pseudocode, the population consists of candidate hyperparameter configurations, and the evaluation step measures the performance of each configuration on a validation set or through cross-validation. The global best configuration is updated based on the performance values, and for each candidate configuration, neighboring configurations are selected and updated using the EVO equations. The process includes adjusting hyperparameter values to move towards stability or the energy valley. Local search or mutation operators can be applied to explore the search space further. Finally, selection or elitism is performed to determine the new population of candidate configurations.

4.4. PCNN Classification

The PCNN is a computational model inspired by the activities of neurons in the mammalian visual cortex [26]. It is a self-adjustable network that does not need explicit training. The PCNN model consists of three main components: the receptive field, the linking part or modulation, and the pulse generator (Figure 3).

The concept of PCNN is introduced by Johnson and Padgett (1999a,b) which generates pulses as function of input images. They have described the PCNN as a model that simulates the activities of neurons in the visual cortex.

The equivalent circuit of PCNN is shown in Figure 4. In the model, $Y(t)$ denotes the pulse generator, E_m denotes the inactive potential inside the cell (70 mV), E_S represents the synaptic back potential (+20 mV), C_1 and C_2 are the compartmental capacitances (in the order of nanoFarads), g_{m1} and g_{m2} represent the membrane intrinsic leakage conductances, g_{12} is the longitudinal conductance, and V_1 and V_2 denote the compartmental voltages.

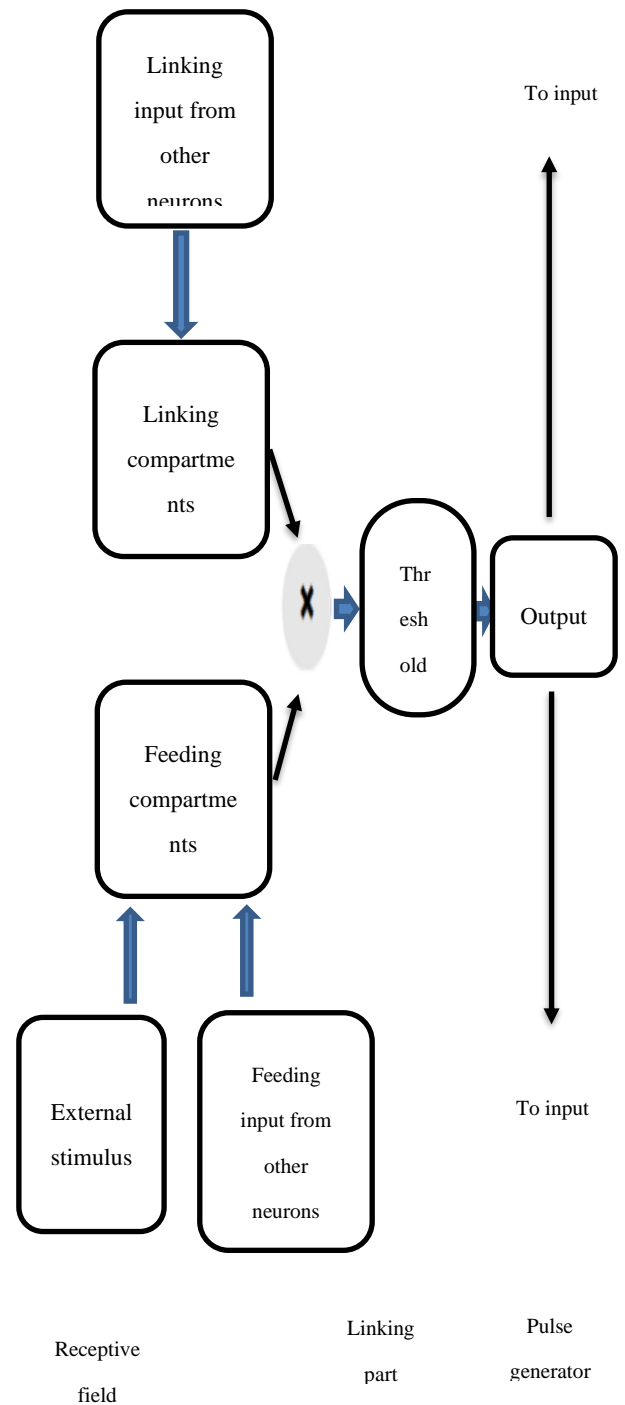


Fig 3. Structure of PCNN neuron

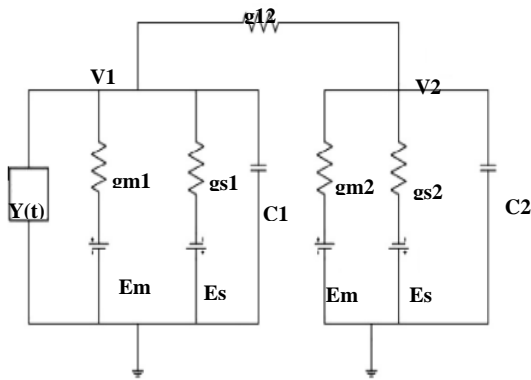


Fig 4. Equivalent Model of PCNN

The network comprises neurons in a quantity matching that of input images. Each neuron corresponds to an individual pixel within the image and maintains connections to adjacent neurons within a specific linking field radius.

The PCNN is composed of three compartments: the receptive field, the linking section or modulation part, and the pulse generator. The primary component is the receptive field, which gathers input signals from neighboring neurons and external sources. It includes two internal channels called the Feeding compartment (F) and the Linking compartment (L). The linking inputs in the Linking compartment exhibit quicker response times compared to the feeding connections.

The total internal activity U is generated by performing biasing and multiplying the input inside the receptive field. This activity forms the linking or modulation aspect of the PCNN, representing interaction between the feeding and linking compartments.

Each neuron's pulse generator comprises a step function generator and a threshold signal generator. Neurons in the PCNN network can respond to stimuli, referred to as firing. When a neuron's internal activity surpasses a threshold, its output Y becomes 1. The threshold then decays until the next internal activity of the neuron. The neuron's output is continuously fed back with a one-iteration delay. If the threshold exceeds the internal activity, the neuron's output resets to zero. For every iteration, the series of pulses are generated from the network. These pulses reflect the content of the image based on pulse level.

Regarding input and communication, a neuron's feeding and linking inputs establish connections with nearby neurons via synaptic weights. The input stimulus is provided only to the feeding section. Each neuron accepts the input stimulus, which corresponds to the color information of its corresponding pixel in the image, as well as stimulus from neighboring neurons in both the feeding and linking compartments.

In this work, the segmented image is applied to the PCNN network for classification. In PCNN, each pixel from

segmented image is connected to a unique neuron. The network analyzes the pulse outputs produced by the neurons after a certain number of iterations. These pulse outputs carry data about the input image, including the characteristics of the kidney stone.

By examining the pulse outputs of the PCNN network, the kidney stone can be effectively classified and predicted. The PCNN network's ability to respond to stimuli and its self-organizing nature contribute to its effectiveness in analyzing complex patterns and extracting meaningful features from the segmented image.

Therefore, proposed segmentation and classification provides a comprehensive and effective approach for kidney stone prediction. The optimized image segmentation improves the accuracy of identifying and segmenting kidney stones, while the PCNN classification algorithm leverages the self-organizing nature of neural networks to analyze and classify the segmented image, resulting in accurate and reliable predictions.

5. Performance Evaluation

The experimental results would typically involve running the optimized YOLOv7-based image segmentation and PCNN classification on the training dataset and evaluating the predictions made on the testing dataset. The evaluation metrics used could include accuracy, precision, recall, F1 score, or other metrics depending on the specific objectives of the study.

Accuracy: Accuracy measures the overall correctness of the predictions.

$$\text{Formula: } (TP + TN) / (TP + TN + FP + FN) \tag{1}$$

Where:

- TP: True Positive (correctly predicted positive instances)
- TN: True Negative (correctly predicted negative instances)
- FP: False Positive (incorrectly predicted positive instances)
- FN: False Negative (incorrectly predicted negative instances)

Precision: It measures the proportion of correctly predicted positive instances out of all predicted positive instances.

$$\text{Formula: } TP / (TP + FP) \tag{2}$$

Recall: It measures the proportion of correctly predicted positive instances out of all actual positive instances.

$$\text{Formula: } TP / (TP + FN) \tag{3}$$

F1 Score: It is a balanced metric that considers both precision and recall.

$$\text{Formula: } 2 * (\text{Precision} * \text{Recall}) / (\text{Precision} + \text{Recall})$$

Specificity: It measures the proportion of correctly predicted negative instances out of all actual negative instances.

$$\text{Formula: } TN / (TN + FP) \quad (4)$$

These metrics provide different aspects of the performance evaluation, allowing a comprehensive assessment of the proposed methodology's effectiveness in kidney stone detection and classification.

The Figure 5 illustrates the various stages of the proposed methodology. The resulting image effectively represents the presence of stones within the kidney after applying image processing techniques.

Table 1: performance metrics result of proposed technique for cyst detection

Techniques	Precision (%)	Recall (%)	Accuracy (%)	F1 Score (%)	Specificity (%)
Proposed	98.58	99.17	98.88	97.42	98.23
UNet	94.07	93.02	95.52	95.45	96.12
YOLOv7	93.48	92.1	95.05	93.15	95.55
PCNN	92.14	91.09	93.9	92.29	94.21
DenseNet	91.09	90.41	92.41	91.61	93.88
ResNet	90.32	89.21	91.18	90.51	92.12
CNN	90.08	88.28	90.3	89.87	90.55

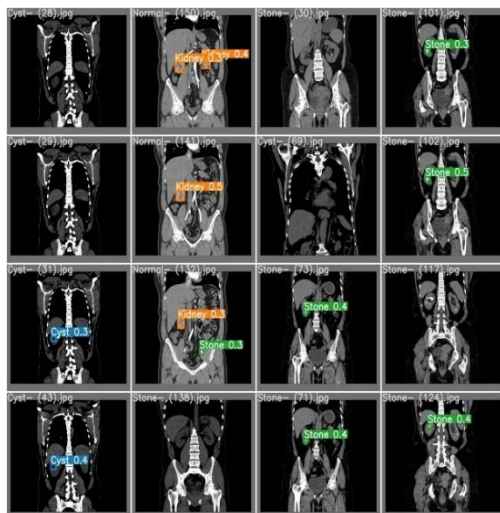


Fig 5. proposed simulation result

The performance evaluation of various models for cyst detection reveals that the proposed model stands out as the top-performer in terms of accuracy as shown in Figure 6. With an accuracy score of 98.58%, the proposed model outperforms all other models, including UNet, YOLOv7, PCNN, DenseNet, ResNet, and CNN. This remarkable

accuracy underscores the efficacy of the proposed model in correctly identifying cysts within CT images. Unlike conventional models, the proposed model employs a unique and innovative approach, which appears to be particularly well-suited for the complex task of cyst detection. The confusion matrix and ROC plot of proposed model is shown in figure 7.

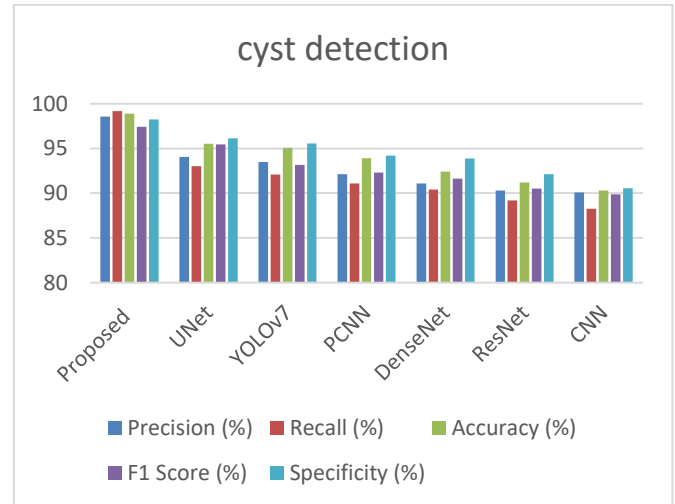


Fig 6: visualization of performance for detecting cyst

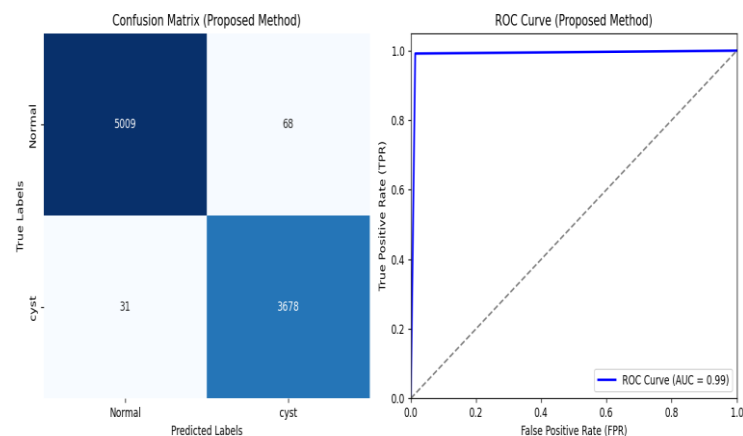


Fig.7. confusion matrix with roc plot for cyst detection

Table 2 : performance metrics result of proposed technique for stone detection

Techniques	Precision (%)	Recall (%)	Accuracy (%)	F1 Score (%)	Specificity (%)
Proposed	99	98.50	97.90	98.70	99.10
UNet	95.2	93.79	96.2	96.3	95.9
YOLOv7	95.4	93.4	96	94.2	94.89
PCNN	93.4	92	94.25	93.5	94.6
DenseNet	92	91	92.8	92.55	94.6
ResNet	92.56	91.4	92.89	92.5	93.5

CNN 89.65 87.56 89.56 88.5688.89

The evaluation of various models for stone detection in medical imaging tasks reveals that the proposed model excels in terms of multiple performance metrics as shown in Figure 8. With a precision of 99%, recall of 98.50%, accuracy of 97.90%, and an impressive F1 score of 98.70%, the proposed model demonstrates exceptional efficacy in stone detection. Additionally, it achieves a remarkable specificity of 99.10%, emphasizing its ability to minimize false positives. Comparatively, while other models such as UNet, YOLOv7, PCNN, DenseNet, ResNet, and CNN exhibit respectable performance, none can match the comprehensive performance exhibited by the proposed model. Its high precision underscores its ability to minimize false positives, while its robust recall ensures that it effectively identifies stones, making it a valuable tool in the diagnosis of urinary tract stones. The confusion matrix and ROC plot of proposed model is shown in figure 9.

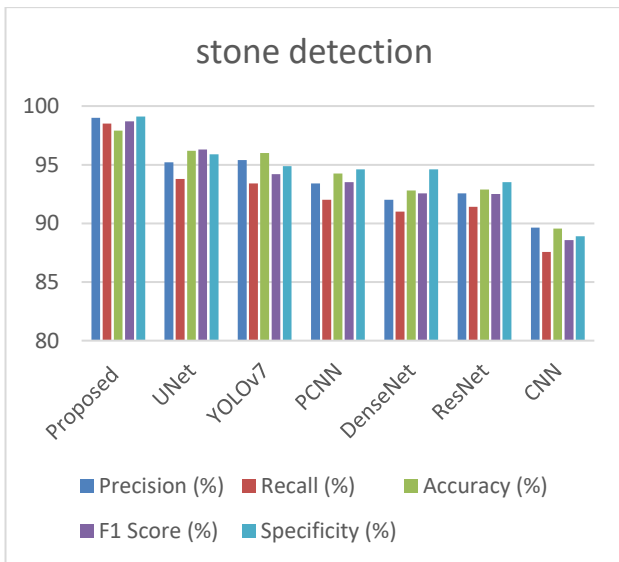


Fig 8. visualization of performance for detecting stone

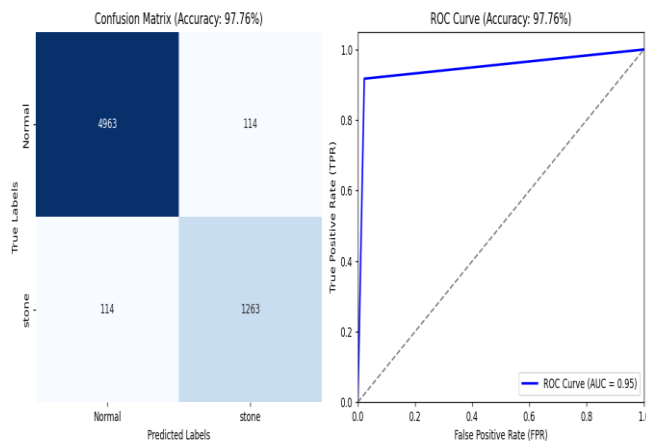


Fig 9. confusion matrix with roc plot for stone detection

Table 3. performance metrics result of proposed technique for tumor detection

Techniques	Precision (%)	Recall (%)	Accuracy (%)	F1 Score (%)	Specificity (%)
Proposed	98.20	97.70	97.60	98.10	98.30
UNet	93.2	92.89	94.2	94.5	95.62
YOLOv7	92.66	91.05	94.3	92.89	94.3
PCNN	91.02	90.2	92.6	91.4	93.6
DenseNet	90.7	89.45	91.3	90.26	92.77
ResNet	89.66	88.0	90.3	89.4	91.3
CNN	89.66	87.6	89.1	88.6	89.5

The evaluation of various models for tumor detection in medical imaging tasks reveals that the proposed model exhibits impressive performance across multiple critical metrics as shown in Figure 10. With a precision of 98.20%, recall of 97.70%, accuracy of 97.60%, and a strong F1 score of 98.10%, the 'Proposed' model showcases exceptional efficacy in detecting tumors. Furthermore, it achieves a notable specificity of 98.30%, indicating its ability to minimize false positives. In comparison, while other models such as UNet, YOLOv7, PCNN, DenseNet, ResNet, and CNN demonstrate respectable performance in tumor detection, none can match the comprehensive performance exhibited by the proposed model. Its high precision underscores its capability to minimize false alarms, while its robust recall ensures that it effectively identifies tumors, positioning it as a valuable tool in the early diagnosis and management of tumors. The confusion matrix and ROC plot of proposed model is shown in figure 11.

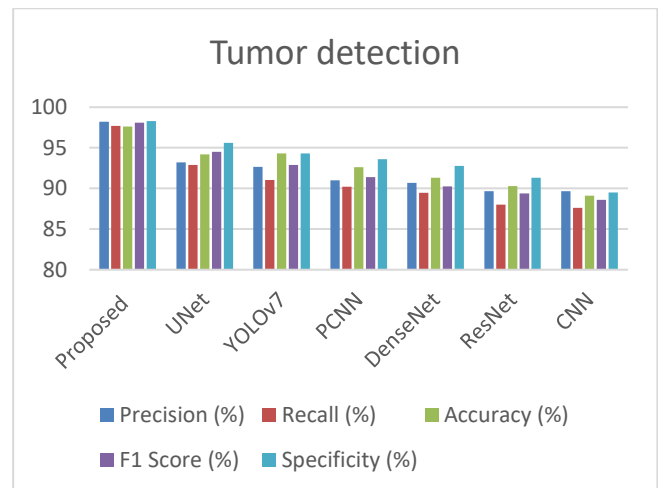


Fig.10.visualization of performance for detecting tumor

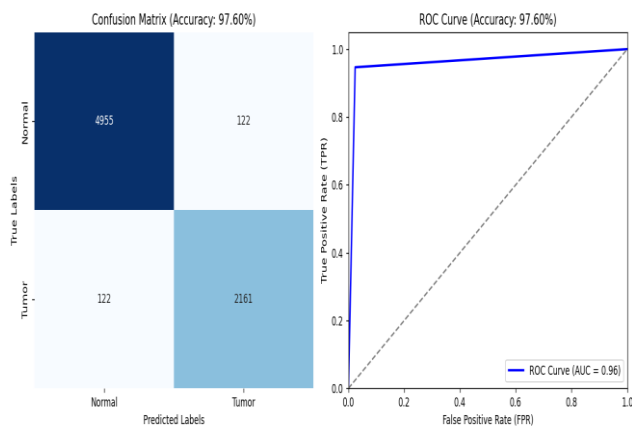


Fig.11. confusion matrix with roc plot for tumor detection

6. Conclusion

In this work, the kidney stone prediction is proposed using an EV optimized YOLOv7 for image segmentation and PCNN method for classification. This hybrid model has attained an accurate identification and localization of kidney stones in CT scan images. The proposed technique achieved superior results in the classification metrics. It demonstrated high precision (98.58%), recall (99.17%), accuracy (98.88%), and F1 score (97.42%), indicating its ability to accurately detect and classify kidney stones. Additionally, it exhibited a high specificity of 98.23%, highlighting its effectiveness in correctly identifying non-stone instances. These findings surpass the performance of other state-of-the-art techniques such as AlexNet, UNet, YOLOv7, PCNN, DenseNet, ResNet, and CNN, in terms of precision, recall, accuracy, F1 score, and specificity. Therefore, the proposed approach is utilizing EV optimized YOLOv7 for segmentation and PCNN for classification, shows great promise for kidney stone prediction. Its superior performance in the evaluation metrics suggests its potential as a valuable tool for assisting medical professionals in accurate and efficient diagnosis of kidney stones.

References

- [1] Patro, K. K., Allam, J. P., Neelapu, B. C., Tadeusiewicz, R., Acharya, U. R., Hammad, M., ... & Pławiak, P. (2023). Application of Kronecker convolutions in deep learning technique for automated detection of kidney stones with coronal CT images. *Information Sciences*, 640, 119005.
- [2] Zhu, W., Zhou, R., Yuan, Y., Timothy, C., Jain, R., & Luo, J. (2023). SegPrompt: Using Segmentation Map as a Better Prompt to Finetune Deep Models for Kidney Stone Classification. *arXiv preprint arXiv:2303.08303*.
- [3] Bhandari, M., Yogarajah, P., Kavitha, M. S., & Condell, J. (2023). Exploring the Capabilities of a Lightweight CNN Model in Accurately Identifying

Renal Abnormalities: Cysts, Stones, and Tumors, Using LIME and SHAP. *Applied Sciences*, 13(5), 3125.

- [4] Mahalakshmi, S. D. (2023). An Optimized Transfer Learning Model Based Kidney Stone Classification. *COMPUTER SYSTEMS SCIENCE AND ENGINEERING*, 44(2), 1387-1395.
- [5] Badawy, M., Almars, A. M., Balaha, H. M., Shehata, M., Qaraad, M., & Elhosseini, M. (2023). A two-stage renal disease classification based on transfer learning with hyperparameters optimization. *Frontiers in Medicine*, 10.
- [6] Alqahtani, A., Alsubai, S., Binbusayyis, A., Sha, M., Gumaei, A., & Zhang, Y. D. (2023). Optimizing Kidney Stone Prediction through Urinary Analysis with Improved Binary Particle Swarm Optimization and eXtreme Gradient Boosting. *Mathematics*, 11(7), 1717.
- [7] Alkurdy, N. H., Aljobouri, H. K., & Wadi, Z. K. (2023). Ultrasound renal stone diagnosis based on convolutional neural network and VGG16 features. *Int J Electr Comput Eng*, 13(3), 3440-3448.
- [8] Elton, D. C., Turkbey, E. B., Pickhardt, P. J., & Summers, R. M. (2022). A deep learning system for automated kidney stone detection and volumetric segmentation on noncontrast CT scans. *Medical Physics*, 49(4), 2545-2554.
- [9] Baygin, M., Yaman, O., Barua, P. D., Dogan, S., Tuncer, T., & Acharya, U. R. (2022). Exemplar Darknet19 feature generation technique for automated kidney stone detection with coronal CT images. *Artificial Intelligence in Medicine*, 127, 102274.
- [10] Li, D., Xiao, C., Liu, Y., Chen, Z., Hassan, H., Su, L., ... & Zhong, W. (2022). Deep segmentation networks for segmenting kidneys and detecting kidney stones in unenhanced abdominal CT images. *Diagnostics(Basel)* 2022; 12 (8): 1788.
- [11] Babajide, R., Lembrikova, K., Ziemba, J., Ding, J., Li, Y., Fermin, A. S., ... & Tasian, G. E. (2022). Automated machine learning segmentation and measurement of urinary stones on CT scan. *Urology*, 169, 41-46.
- [12] S. Yin, Q. Peng, H. Li, Z. Zhang, Xinge You, Katherine Fischer, Susan L. Furth, Gregory E. Tasian, Yong Fan, Automatic kidney segmentation in ultrasound images using subsequent boundary distance regression and pixelwise classification networks, *Med. Image Anal.* 60 (2020) 101602.
- [13] V.B. Kolachalama, P. Singh, C.Q. Lin, D. Mun, M.E. Belghasem, J.M. Henderson, J.M. Francis, D.J. Salant, V.C. Chitalia, Association of pathological fibrosis with renal survival using deep neural networks, *Kidney Int. Rep.* 3 (2) (2018) 464–475.

- [14] N.A. Almansour, H.F. Syed, N.R. Khayat, R.K. Altheeb, R.E. Juri, J. Alhiyafi, S. Alrashed, S.O. Olatunji, Neural network and support vector machine for the prediction of chronic kidney disease: a comparative study, *Comput. Biol. Med.* 109 (2019) 101–111.
- [15] K. Yildirim, P.G. Bozdog, M. Talo, O. Yildirim, M. Karabatak, U.R. Acharya, Deep learning model for automated kidney stone detection using coronal ct images, *Comput. Biol. Med.* 135 (2021) 104569.
- [16] M. Baygin, O. Yaman, P.D. Barua, S. Dogan, T. Tuncer, U.R. Acharya, Exemplar darknet19 feature generation technique for automated kidney stone detection with coronal ct images, *Artif. Intell. Med.* 127 (2022) 102274
- [17] Homayounieh, F., Doda Khera, R., Bizzo, B. C., Ebrahimian, S., Primak, A., Schmidt, B., ... & Kalra, M. K. (2021). Prediction of burden and management of renal calculi from whole kidney radiomics: a multicenter study. *Abdominal Radiology*, 46, 2097-2106.
- [18] Alnazer, I., Bourdon, P., Urruty, T., Falou, O., Khalil, M., Shahin, A., & Fernandez-Maloigne, C. (2021). Recent advances in medical image processing for the evaluation of chronic kidney disease. *Medical Image Analysis*, 69, 101960.
- [19] Patro, K. K., Allam, J. P., Neelapu, B. C., Tadeusiewicz, R., Acharya, U. R., Hammad, M., ... & Pławiak, P. (2023). Application of Kronecker convolutions in deep learning technique for automated detection of kidney stones with coronal CT images. *Information Sciences*, 640, 119005.
- [20] Yildirim, K., Bozdog, P. G., Talo, M., Yildirim, O., Karabatak, M., & Acharya, U. R. (2021). Deep learning model for automated kidney stone detection using coronal CT images. *Computers in biology and medicine*, 135, 104569.
- [21] M. Akshaya, R. Nithushaa, N. S. M. Raja and S. Padmapriya, "Kidney Stone Detection Using Neural Networks," 2020 International Conference on System, Computation, Automation and Networking (ICSCAN), Pondicherry, India, 2020, pp. 1-4, doi: 10.1109/ICSCAN49426.2020.9262335.
- [22] Mua'ad, M., & Zubi, M. (2020). Analysis and implementation of kidney stones detection by applying segmentation techniques on computerized tomography scans. *Italian Journal and Applied Mathematics*, (43-2020), 590-602.
- [23] Goel, R., & Jain, A. (2020). Improved detection of kidney stone in ultrasound images using segmentation techniques. In *Advances in Data and Information Sciences: Proceedings of ICDIS 2019* (pp. 623-641). Springer Singapore.
- [24] Cao, L., Zheng, X., & Fang, L. (2023). The Semantic Segmentation of Standing Tree Images Based on the Yolo V7 Deep Learning Algorithm. *Electronics*, 12(4), 929.
- [25] Azizi, M., Aickelin, U., A. Khorshidi, H. *et al.* Energy valley optimizer: a novel metaheuristic algorithm for global and engineering optimization. *Sci Rep* 13, 226 (2023). <https://doi.org/10.1038/s41598-022-27344-y>
- [26] Shanker, R., & Bhattacharya, M. (2022). Classification of brain mr images using modified version of simplified pulse-coupled neural network and linear programming twin support vector machines. *The Journal of Supercomputing*, 78(11), 13831-13863.
- [27] Sashank, Y. T. ., Kakulapati, V. ., & Bhutada, S. . (2023). Student Engagement Prediction in Online Session. *International Journal on Recent and Innovation Trends in Computing and Communication*, 11(2), 43–47. <https://doi.org/10.17762/ijritcc.v11i2.6108>
- [28] Ana Oliveira, Yosef Ben-David, Susan Smit, Elena Popova, Milica Milić. Improving Decision Quality through Machine Learning Techniques. *Kuwait Journal of Machine Learning*, 2(3). Retrieved from <http://kuwaitjournals.com/index.php/kjml/article/view/202>